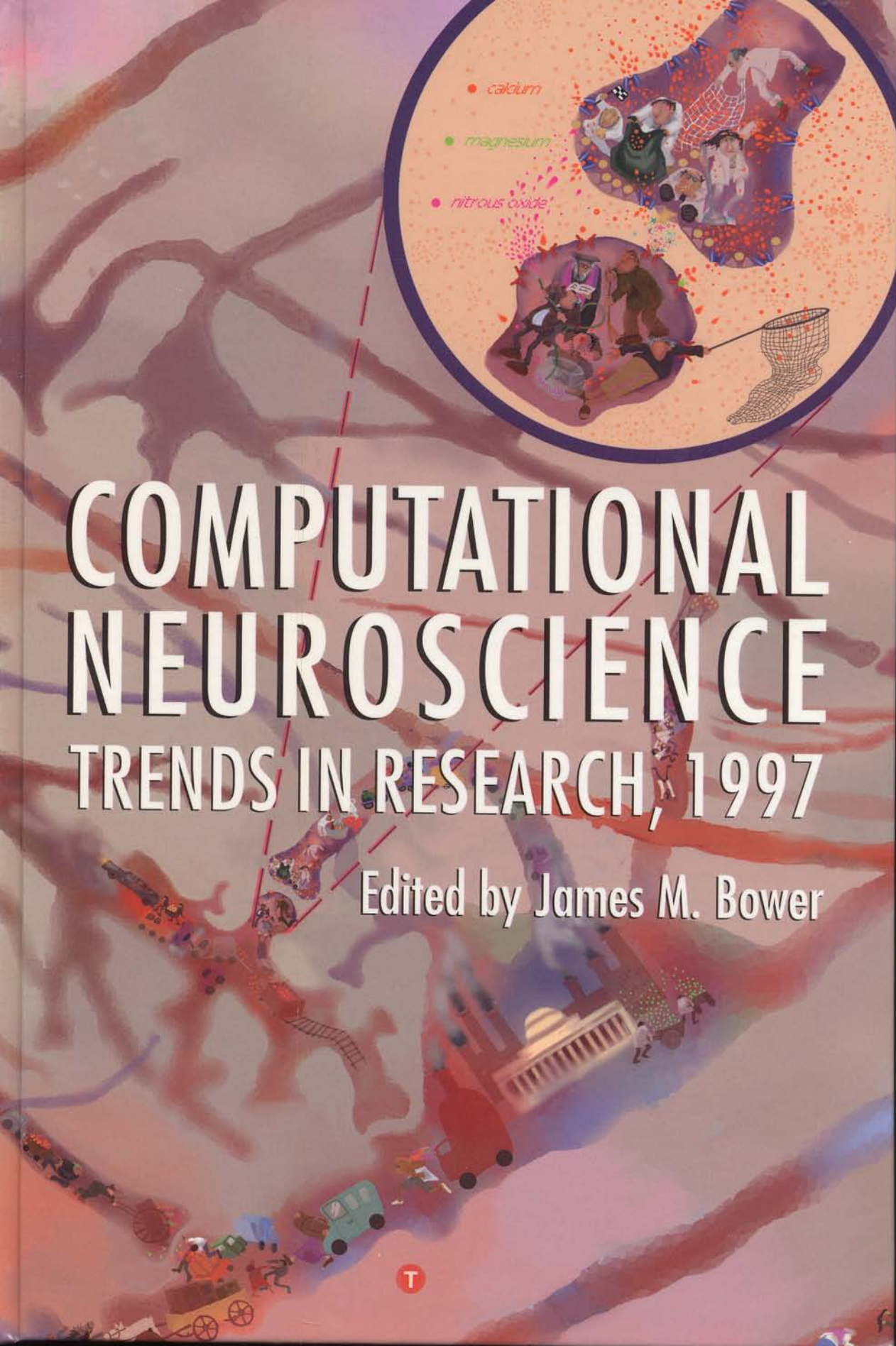

COMPUTATIONAL NEUROSCIENCE

TRENDS IN RESEARCH, 1997

Edited by James M. Bower

Computational Neuroscience

Trends in Research, 1997

Edited by

James M. Bower
California Institute of Technology
Pasadena, California

Plenum Press • New York and London

CONTENTS

ESTIMATION OF SIGNAL CHARACTERISTICS DURING ELECTROLOCATION FROM VIDEO ANALYSIS OF PREY CAPTURE BEHAVIOR IN WEAKLY ELECTRIC FISH

Malcolm A. MacIver, John L. Lin, and Mark E. Nelson

The Neuroscience Program and
Beckman Institute for Advanced Science and Technology
University of Illinois
Urbana-Champaign Urbana, Illinois 61801

INTRODUCTION

Weakly electric fish can actively influence the strength and spatiotemporal patterns of incoming electrosensory signals by controlling the velocity and orientation of their body and by adjusting the gain and filtering properties of neurons in the electrosensory lateral line lobe (ELL) via descending control (review: Bastian 1995). To better understand the signal conditions under which the active electric sense normally operates, we have undertaken a set of behavioral studies aimed at characterizing how electric fish use their electrosensory system to locate and capture small prey. Key questions we are pursuing include the range of detectability for small prey; the typical signal magnitude of prey within this range; the typical velocity of the prey relative to the receptor array; the movement strategies of the fish during prey search, localization, and strike phases of behavior; and the spatiotemporal patterns of receptor activation during prey capture behavior and how these patterns relate to the filtering properties of sensory neurons in the ELL. Answers to these questions will be used to guide and constrain our electrophysiological and neural modeling studies.

In general, we find that under natural conditions the electrosensory system operates at signal levels that are much lower than those typically used in electrophysiological studies to characterize the system. We hope that by focusing our attention on the signal processing required to extract small natural signals, we can gain a better understanding of the active components of sensory acquisition and of the adaptive filtering task of the ELL. In this paper we describe how we record and analyze the sensory acquisition behavior of a South American weakly electric fish (*Apteronotus albifrons*) during capture of small aquatic prey *(Daphnia magna*), and how we estimate the spatiotemporal pattern of transdermal potential and afferent firing rate changes during this challenging electrosensory task.

Computational Neuroscience
edited by Bower, Plenum Press, New York, 1997

METHODS

These studies were conducted with adult *Apteronotus albifrons* (black ghost) weakly electric knife fish, 12–16 cm in length, maintained in water of 250 ± 25 mS conductivity at 27 ± 1.0°C, and pH 6.9 ± 0.2, on a 12-hour light/dark cycle. For prey we used mature (2–3 mm) *Daphnia magna* (water fleas) that were cultured in our laboratory for this purpose.

Estimation of Prey Detection Distance

Behavioral Data Acquisition. Prey search and prey capture behavior was recorded within an infrared videotaping setup (see Figure 1). Fish were housed in a rectangular Plexiglas aquarium (77 x 30 x 20 cm) with a central area partitioned from the rest of the aquarium to form an arena (40 x 30 x 20 cm) which constrained fish-prey interactions to the region imaged by our video cameras. Four fish were held in individual holding bays that were electrically insulated from the arena in which behavior was observed; prior to recording, one fish was allowed into the recording arena through a Plexiglas door. Prey were introduced into the aquarium one at a time using a narrow tube with minimal mechanical disturbance and without introduction of visible light.

Infrared Videotaping. For this study we developed an infrared videotaping setup (Figure 1A) to record behavior that has no visually-mediated component. Two black and white cameras provided top and side views. The two video cameras were coupled and their output sent to a commercial video splitter to merge the top and side views of the tank. The merged images were recorded on videotape. Infrared illumination was provided by two custom-fabricated IR light sources, each consisting of 100 high-intensity infrared diodes (radiant power 35 mW, 880 nm). The illuminators, cameras, and aquarium were within a light-tight enclosure.

Video Digitizing and Trajectory Reconstruction. Videotaped records of prey capture behavior were visually scanned to identify segments to be digitized. Segment selection was based on several criteria: 1) the segment included an orienting response toward the

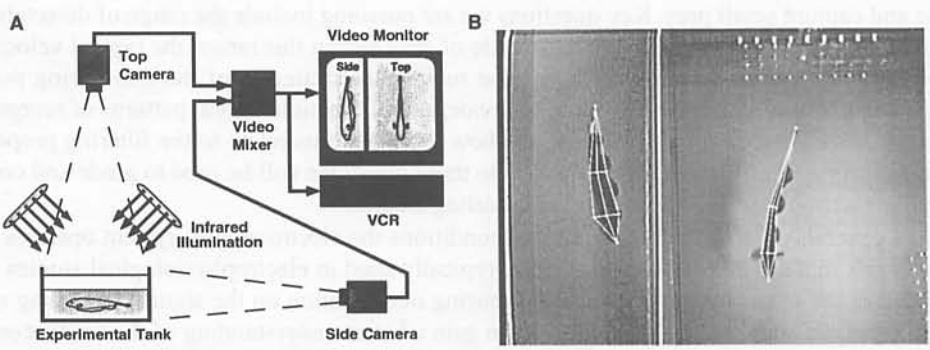

Figure 1. Behavioral recording setup and video reconstruction. (A) Schematic diagram of two-camera infrared video setup. The experimental tank and cameras were housed within a light-tight enclosure. (B) One picture of raw video data with an illustrative wireframe model overlaying the fish. The actual wireframe mesh used has 7 nodes per (top and side) view to represent the fish, and 1 node to represent the prey.

prey, either a lunge or a change in swimming pattern near the prey 2) the prey had to be located on the sides of the fish closest to the top and side view cameras, as otherwise our view of the prey was blocked; 3) the trajectory of the fish must have been at least 4 cm away from the bottom and sides of the tank, to minimize distortions in the fish's electric field that occur near boundaries. We used a Peak Performance Technologies motion measurement system for digitizing videotape of behavior. The sampling rate was 60 pictures per second, where a picture is one video field with the alternate scan lines interpolated. For each digitized image, a wireframe mesh was constructed to indicate the fish body position. The fish mesh had 7 nodes in each view (top and side), corresponding to the tip of the snout, the right and left pectoral fins at their anterior insertion points, a ventral and dorsal surface point midway between the pectoral fins, the midpoint of the fish on the central long axis, and the tip of the caudal fin. Figure 1B shows a typical picture of the raw video data used during digitization, overlaid with a sample wireframe mesh. A single point was used in each view to mark the location of the prey. The coordinates of the wireframe nodes were then used to reconstruct the 3-D trajectory of fish and prey during prey search, detection, and capture phases of behavior.

Data Analysis and Interpretation. Data analysis was carried out using MATLAB running on Sun workstations. Reconstructed node trajectories were digitally low-pass filtered to attenuate jitter due to small variations in manual point placement across pictures, then combined to reconstruct the 3-D trajectories of the fish and prey. The trajectories were analyzed to extract prey position, prey velocity, fish position, fish velocity, fish acceleration, the distance between the prey and the closest point on the fish body, and the distance between the prey and the fish mouth. The putative time of detection was identified using two criteria: 1) a longitudinal acceleration peak exceeding a threshold value, and 2) an orienting response which was terminated with a lunge towards the prey. Analysis of post-detection events was carried out using observations of the raw videotape as well as quantitative measures obtained from the digitized trajectories.

Reconstruction of Spatiotemporal Patterns of Transdermal Potential and Afferent Activity. When visualizing changes in transdermal potential we represented the unfolded bilateral electroreceptor surface of the fish as an idealized rectangular grid (Figure 3). The projected coordinates of the *Daphnia* were transformed into this representation. When estimating changes in transdermal potential, we treat the *Daphnia* as a 2 mm spherical insulating object. Based on the physics of electrosensory image formation (Rasnow, 1996) we then estimated spatial spread and signal intensity of the electrosensory "shadow" cast upon the fish at each time frame and calculated the transdermal potential change at each point on the idealized electroreceptor surface. We then used the estimated transdermal potential as the input to a linear-nonlinear cascade model of primary electrosensory afferent response dynamics (Xu et al. 1994) to estimate the associated changes in P-type tuberous electrosensory afferent activity during the prey-capture sequence.

RESULTS AND DISCUSSION

We reconstructed the 3-D trajectories of 81 prey capture sequences and extracted estimates of acceleration, velocity and distance of closest approach from each sequence. Figure 2A show a sample of how these parameters vary during a typical sequence. Initially the fish is swimming with a relatively constant forward velocity of about 10 cm/s,

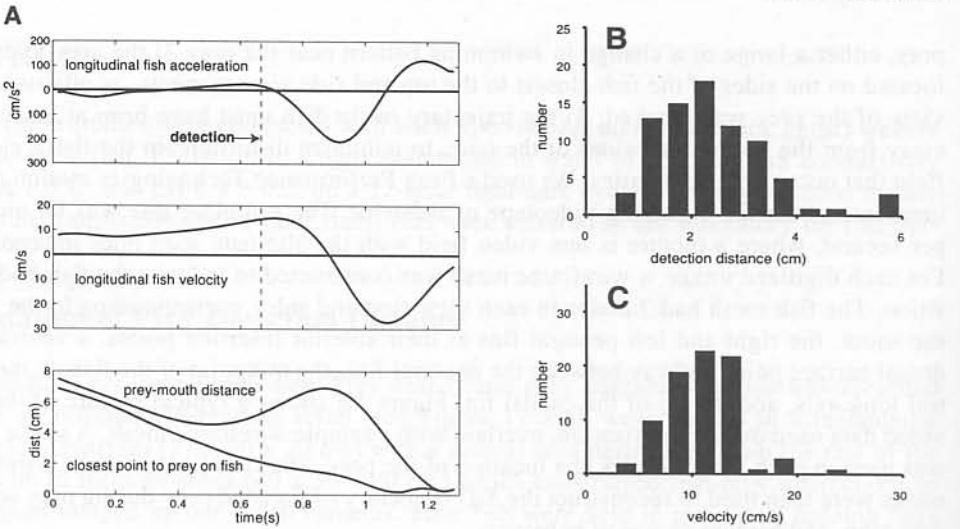

Figure 2. (A) The longitudinal acceleration, velocity, and distance between prey and fish during a typical prey capture. The estimated time of prey detection is indicated by the dashed vertical line at t = 0.7 s (B) Distance between prey and closest point on fish body surface at time of detection (mean 2.4 cm, s.d. 1.1 cm, N=81). (C) Relative velocity between fish and prey at time of detection (mean 11 cm/s, s.d. 3.6 cm/s, N=81).

then there is an abrupt longitudinal deceleration (t = 0.7–1.0 s) and longitudinal velocity reversal (t = 0.9 s) as the fish backs up to capture a *Daphnia* that has been detected by electroreceptors on the trunk. The abrupt deceleration and velocity reversal are characteristic of most prey strike sequences we have recorded. Based on analysis of the longitudinal acceleration profile we estimate that prey detection occurred near the onset of the deceleration at t = 0.7 s (dashed vertical line). At the time of detection, the fish was moving with a forward velocity of 14.6 cm/s and the prey was approximately 2.1 cm from the closest point of the fish's body, which was in the mid-trunk region for this detection event. Preliminary analysis of 81 such sequences indicates that the typical detection distance for small prey (*Daphnia*, 2–3mm diameter) is approximately 2.4 cm (Figure 2B); the typical fish-prey velocity at the time of detection is about 11 cm/s (Figure 2C).

From the reconstructed trajectories we then estimate the change in transdermal potential at 100 ms intervals as shown in Figure 3A. Based on the physics of electric image formation for spherical objects (Rasnow 1996) and approximating the *Daphnia* as a perfect insulator due to its non-conducting carapace, we compute the peak amplitude and full-width at half maximum for the electric image the Daphnia casts on the electroreceptor array at each time point. Figure 3A shows the resulting pattern of transdermal potential change for the final half (0.6–1.2 s) of the prey capture sequence shown in Figure 2A. Note that the electric image is weak and diffuse at the beginning of the sequence and becomes both more intense and more tightly focused as the *Daphnia* gets closer to the electroreceptor array. At the time of detection (t = 0.7 s), the estimated peak transdermal potential modulation is about 0.1 μV RMS and just before prey capture (t = 1.2 s) the peak modulation is about 5.0 μV RMS.

Based on the estimated transdermal potential change, we then compute the corresponding change in afferent firing rate based on a model of P-type electrosensory afferent response dynamics that we have developed (Xu et al., 1994). The afferent model is a linear-nonlinear cascade model consisting of a second order linear model that describes the

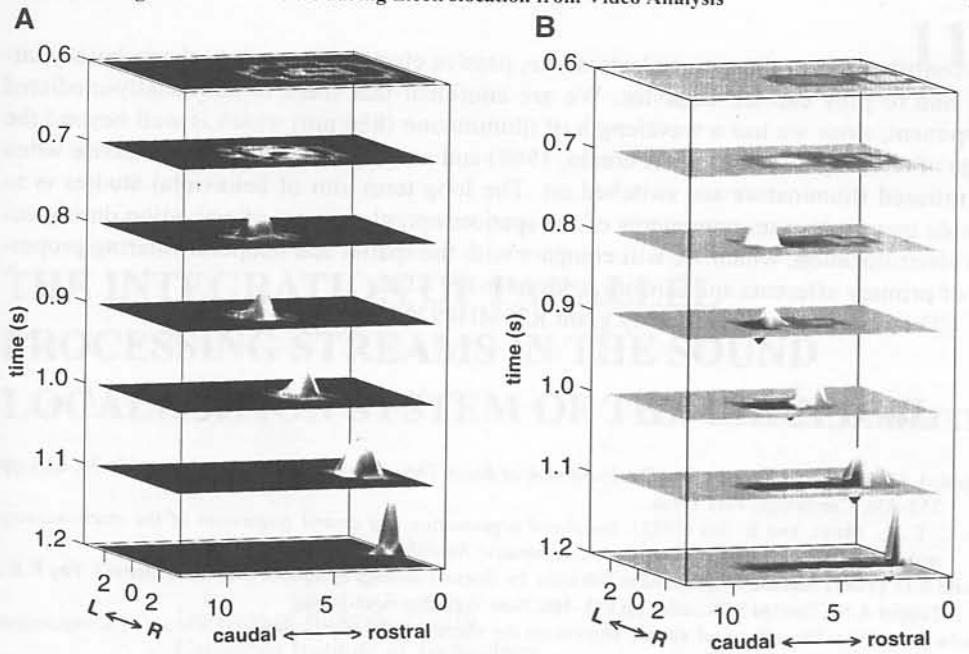

Figure 3. (A) Spatiotemporal pattern of the change in transdermal potential during the last segment (0.6–1.2 s) of the prey capture event shown in Figure 2. (B) Corresponding pattern of P-type afferent firing rate changes. Note the trailing depression in firing rate in planes from t=0.8 s to the end of the sequence (dark patches). This is due to the depression in afferent firing rate that occurs at the offset of a stimulus.

frequency dependence of the gain and phase of the response, in series with a static nonlinearity that incorporates the effects of firing rate rectification and saturation. Figure 3B shows the change in afferent firing rate corresponding to the change in transdermal potential shown in Figure 3A. At the time of detection (t = 0.7 s), the estimated peak rate modulation on an individual afferent is only 0.2 spike/s, but since the electric image is spatially diffuse, approximately 600 P-type electrosensory afferents are influenced simultaneously. One unexpected result from this analysis is the trailing suppression of afferent firing rate (dark regions in Figure 3B) as the stimulus moves across the surface of the fish's skin. This trail of suppressed activity, which arises from the response dynamics of the afferents, provides a short-term spatial memory of the trajectory history which could possibly be used centrally to aid in target tracking computations.

Using natural prey-capture sequences to estimate electrosensory signal characteristics has provided us with a much better understanding of the conditions under which the electrosensory system normally operates. While *Daphnia* are probably not a prey item in the native habitat of *A. albifrons*, they are similar in size to prey found in stomach-content analyses of this species in their natural environment (M. Hagedorn 1996, unpublished data). We have not yet demonstrated that prey detection is mediated by the active electric sense alone, since we do not know the extent to which sensory modalities other than the tuberous (active) electrosensory system, most importantly the mechanosensory lateral line and low-frequency ampullary (passive) electrosensory system, may contribute to prey detection and localization. In many cases, the apparent detection event was followed by backward scanning, dorsal edge scanning, and tail-bending behaviors, which are suggestive of active electrolocation. We are about to undertake a study that will assess the rela-

tive contributions of the active electrosense, passive electrosense and mechanosensory lateral line to prey capture behavior. We are confident that there is no visually-mediated component, since we use a wavelength of illumination (880 nm) which is well beyond the range of teleost photoreceptors (Fernald, 1988) and our fish show no startle response when the infrared illuminators are switched on. The long term aim of behavioral studies is to provide quantitative measurements of the spatiotemporal patterns of activation during active electrolocation, which we will compare with the spatial and temporal filtering properties of primary afferents and sensory neurons in the ELL.

This research is supported by grant R29MH49242 from NIMH.

REFERENCES

Bastian, J. (1995) Electrolocation. In: *The Handbook of Brain Theory and Neural Networks*, (Arbib M. ed.), pp 352–356. Cambridge: MIT Press.

Carr, C. E., L. Maler, and E. Sas (1982). Peripheral organization and central projections of the electrosensory nerves in Gymnotiform fish. *Journal of Comparative Neurology* (2): 139–153.

Fernald R.D. (1988) Aquatic adaptations in fish eyes. In: *Sensory Biology of Aquatic Animals* (Atema J, Fay R.R., Popper A.N., Tarolga W.N., eds), pp 433–466. New York: Springer-Verlag.

Rasnow B. (1996) The effects of simple objects on the electric field of *Apteronotus*. *Journal of Comparative Physiology A* 178:397–411.

Xu, Z. and Payne, J.R. and Nelson, M.E. (1994). System identification and modeling of primary electrosensory afferent response dynamics. *Computation in Neurons and Neural Systems*, Eeckman, F., ed. Kluwer Academic Press, 197–202.